Revised Manuscript: Ms. Ref. No.: CATTOD-D-19-00487

Catalytic reduction of nitrate in water over alumina-supported nickel catalyst toward purification of polluted groundwater

Marina Kobune [a], Dai Takizawa [a], Jun Nojima [a], Ryoichi Otomo [b], Yuichi Kamiya [b,*]

[a] *Graduate School of Environmental Science, Hokkaido University, Kita 10 Nishi 5, Sapporo 060-0810, Japan.*

[b] *Faculty of Environmental Earth Science, Hokkaido University, Kita 10 Nishi 5, Sapporo 060-0810, Japan.*

Corresponding author:

* *Yuichi Kamiya*

E-mail: kamiya@ees.hokudai.ac.jp

Tel: +81-11-706-2217

Abstract

Pollution of groundwater with NO_3^- is a serious problem in the world. While catalytic reduction of NO_3^- over Pd-bimetallic catalysts including Cu-Pd and Sn-Pd is a promising method for purification of the groundwater, the use of precious metal is a major obstacle for practical applications. In the present study, we applied Ni/Al_2O_3 for the catalytic reduction of NO_3^- and compared the catalytic performance with that of unsupported Ni catalyst. The reaction rate over 5 wt.% Ni/Al_2O_3 was about 5 times higher than that of the unsupported Ni catalyst, based on unit weight of catalyst. While the unsupported Ni catalyst was completely deactivated in low partial pressure of H_2 (= 0.75 atm) and high concentration of NO_3^- (= 800 ppm), Ni/Al_2O_3 was still active even under less reductive conditions ($[NO_3^-]_0$ = 800 ppm and $P(H_2)$ = 0.5 atm). The unsupported Ni catalyst had the Ni^0 particles formed by the reduction of NiO with H_2 at 310 – 420 ºC. On the other hand, 5 wt.% Ni/Al_2O_3 possessed the Ni^0 particles formed from $NiAl_2O_4$ on Al_2O_3 by the reduction with H_2 above 450 ºC. It is plausible that those Ni^0 particles had different properties, giving different catalytic properties. The Ni loadings for Ni/Al_2O_3 had a significant impact on the catalytic properties. The reaction orders with respect to both NO_3^- and H_2 were 0.8 for 5 wt.% Ni/Al_2O_3, while those were 0 and –0.2, respectively, for 10 wt.% Ni/Al_2O_3. On 10 wt.% Ni/Al_2O_3, there were two kinds of the Ni^0 particles, which were formed by low (310 420 ºC) and high (450 ºC ~) temperature H_2 reductions. Unlike the Pd-bimetallic catalysts, the reduction of NO_3^- over Ni/Al_2O_3 did not proceed through NO_2^-.

Keywords: Nitrate reduction; Ni/Al_2O_3; Base metal catalyst; Water purification

1. Introduction

Pollution of groundwater with nitrate (NO_3^-), which is caused by overuse of agricultural nitrogen fertilizers, inappropriate disposal of livestock excreta, and leakage of industrial and domestic effluents, is a serious problem in the world [1, 2]. Drinking water containing high concentration of NO_3^- poses a health hazard including methemoglobinemia [2]. In addition, formation of carcinogenic nitrosamine may occur in human body [3]. Thus, the World Health Organization (WHO) recommends that the concentration of NO_3^- in drinking water should be below 50 mg L^{-1} [3]. Since infant is highly susceptible to NO_3^-, less than 3 mg L^{-1} is strongly recommended [3].

So far, various treatment technologies including biological [4] and physical methods such as adsorption [5], ion exchange [6] and reverse osmosis [7] have been applied for the purification of nitrate-polluted groundwater. However, each of them has problems; in the former being strict treatment conditions, risk of contamination by pathogenic bacteria and slow treatment rate [4]. In the latter, not only regeneration of ion exchange resins and semipermeable membranes is required at regular intervals but also the polluted water generated in the course of the regeneration should be properly treated [8].

Catalytic hydrogenation of NO_3^- to N_2 over a solid catalyst has attracted much attention as a method to decompose NO_3^- to harmless product with substantial reaction rate [9-32], being, for example, 8.3 mmol h^{-1} g^{-1} over Sn-Pd/Al_2O_3 [31]. The reaction gives NH_3 (or NH_4^+ if solution is acidic) as a possible product besides N_2 (eqs. 1 and 2).

$$NO_3^- + 5/2H_2 \rightarrow 1/2N_2 + 2H_2O + OH^- \quad (1)$$

$$NO_3^- + 4H_2 \rightarrow NH_3 + 2H_2O + OH^- \quad (2)$$

Thus, the catalysts should have not only high activity but also high selectivity to N_2 suppressing formation of NH_3 (or NH_4^+). Since the discovery by Hörold et al. [9], supported bimetallic catalysts, which are the combination of precious metal (Pd and Pt) and base metal (Cu, Sn and In), have been intensively studied. So far, such bimetallic catalysts showing high activity, high selectivity and high durability have been developed [10-32]. Some Pd-bimetallic catalysts were applied for the treatment of actual groundwater. While the reaction rates in actual groundwater fell to about one-fifth of that in an aqueous NO_3^- solution, the catalysts still enabled to purify the groundwater [31]. However, the use of precious metals is a major obstacle for practical applications due to their expensiveness. Thus, development of catalysts composed of only inexpensive base metals is keenly desired for practical applications.

Nickel is a less expensive base metal and is known to activate H_2. Hence, it is used as industrial catalysts for hydrogenation of alkene, fats, and aromatics [33-36]. However, there are only few reports on the application of Ni catalysts for the reduction of NO_3^- in water and most catalysts except for Raney Ni [37-39] did not show any activity for the reaction [40]. Mikami et al. investigated catalytic hydrogenation of NO_3^- in water using a Raney Ni catalyst and found that despite base metal, it showed extremely high activity, which was more than 100 times higher than that of supposed Pd-Cu catalyst

[37-39]. Furthermore, they modified Raney Ni with small amount of Zr or Pt so as to improve the catalytic activity [37-39]. However, undesirable NH_3 (or NH_4^+) was the predominant product over Raney Ni irrespective of the modifications.

In general, the use of a carrier like Al_2O_3 for supported metal catalysts increases the catalytic activity brought by high dispersion of the metal particles [41]. In addition, it is known that selectivity is also altered by the supporting owing to changes in exposed crystal face and particle shape, increase in the number of highly unsaturated coordination sites, electronic interaction between metal and support, and involvement of the interface between support and metal particle in the catalytic reaction [41-46]. Therefore, in this study, we investigated catalytic reduction of NO_3^- with H_2 in water over alumina-supported Ni catalyst and compared the catalytic performance with that of unsupported Ni catalyst, which was obtained by reduction of NiO with H_2. Furthermore, the influence of Ni loading for Ni/Al_2O_3 on the nature of Ni species and catalytic properties was investigated.

2. Experimental

2.1. Preparation of catalysts

Alumina-supported Ni catalyst was prepared by an impregnation method. $Ni(NO_3)_2 \cdot 6H_2O$ (FUJIFILM Wako Pure Chemical Co., 0.255 and 0.510 g for 5 and 10 wt.% Ni, respectively) was dissolved in Milli-Q water (30 mL). To the solution, Al_2O_3 (Nippon Aerosil Co., Ltd., AEROXIDE®,

Alu C, 1.0 g, 100 $m^2 g^{-1}$) was added and the suspension was moderately stirred at room temperature for 30 min. The suspension was then evaporated to dryness at 50 °C by using a rotary evaporator. The resulting solid was dried in air at 100 ºC overnight and calcined in air at 500 ºC for 3 h. The loading amounts of Ni on Al_2O_3 were adjusted to 5 and 10 wt.%. Just before the reduction of NO_3^-, the catalyst was reduced with H_2 at 600 ºC for 1 h. For the preparation of unsupported Ni catalyst, $Ni(NO_3)_2 \cdot 6H_2O$ was calcined in air at 500 ºC for 3 h and the resulting NiO was reduced in the similar manner to that for Ni/Al_2O_3. The BET surface areas of 5 and 10 wt.% Ni/Al_2O_3 were 112 and 102 $m^2 g^{-1}$, respectively. The surface area of the unsupported Ni catalyst was too low to be measured from a N_2 adsorption isotherm and thus was below 1 $m^2 g^{-1}$. Since the Ni/Al_2O_3 catalysts with Ni loadings less than 5 wt% were unsuitable for characterization including powder X-ray diffraction and temperature-programmed reduction with H_2 due to low Ni loadings while they showed the catalytic performances similar to 5 wt% catalyst, we chose 5 wt.% Ni/Al_2O_3 as a typical sample for low Ni loadings.

Raney Ni catalyst was prepared from Ni-Al alloy (50 wt.% Ni, FUJIFILM Wako Pure Chemical Co.) according to the literature [47]. Ni-Al alloy (0.4 g) was added to an aqueous NaOH solution (25%, 40 mL) while maintaining the temperature below 50 ºC. Then the suspension was treated at reflux temperature for 90 min with vigorous stirring. After the suspension was cooled to room temperature, the supernatant was decanted. Then the obtained powder was washed with Milli-Q water many times until the supernatant was neutral.

2.2. Catalytic reduction of NO_3^- with H_2 in water

Aqueous NO_3^- solutions with different concentrations of 1200, 2400 and 4800 ppm, which correspond to 19.38, 38.76 and 77.52 mmol L^{-1}, respectively, were prepared by dissolving appropriate amount of KNO_3 (FUJIFILM Wako Pure Chemical Co.) in Milli-Q water. The solution (200 mL) was purged with a stream of N_2 (30 mL min^{-1}) for 90 min to expel dissolved air prior to the catalytic reaction.

Ni/Al_2O_3 (0.2 g), which was reduced in advance by the manner described in 2.1, was added to Milli-Q water (100 mL) in a round-bottom flask (200 mL), into which H_2 was flown at 30 mL min^{-1} for 90 min. To this suspension the aqueous NO_3^- solution (20 mL, 2400 ppm) was added to obtain the reaction solution (120 mL) with 400 ppm NO_3^-. The time, at which the aqueous NO_3^- solution was added, was regarded as a start time for the reaction. To obtain the reaction solutions with 200 and 800 ppm NO_3^-, the aqueous NO_3^- solutions with 1200 and 4800 ppm NO_3^-, respectively, were used instead of the solution with 2400 ppm NO_3^-. Temperature of the reaction solution was kept at 40 ºC throughout the catalytic reaction. Since Ni/Al_2O_3 was easily deactivated by contact with air, the reactor was tightly closed up with a rubber septum and the reaction solution was taken out through the septum by using a syringe to prevent entry of air into the reactor. The reaction solution was analyzed by using ion chromatographs (IC-2001, Tosoh) to determine the concentrations of NO_3^-, NO_2^- and NH_4^+. For anion

(NO_3^- and NO_2^-) analysis, a TSK gel Super IC-AZ column (Tosoh) was used with an aqueous solution of $NaHCO_3$ (2.9 mmol L^{-1}) and Na_2CO_3 (3.1 mmol L^{-1}) as eluent. For cation (NH_4^+) analysis, a TSK gel Super IC-Cation 1/2 HR column (Tosoh) was used with an aqueous solution of methane sulfonic acid (2.2 mmol L^{-1}) and 18-crown-6 (1.0 mmol L^{-1}) as eluent. The conversion of NO_3^- and selectivities were calculated by using the following equations (eqs. 3 and 4).

$$\text{Conversion of } NO_3^-(\%) = \frac{\text{Concentration of consumed } NO_3^-}{\text{Initial concentration of } NO_3^-} \times 100 \quad (3)$$

$$\text{Selectivity to } NO_2^-(\text{or } NH_4^+)(\%) = \frac{\text{Concentration of formed } NO_2^-(\text{or } NH_4^+)}{\text{Concentration of consumed } NO_3^-} \times 100 \quad (4)$$

Because analysis of gaseous products was not performed in this study, the selectivity to them was calculated by subtracting the selectivities to NO_2^- and NH_4^+ from 100%.

2.3. Characterization

Temperature-programmed reduction profiles of Ni catalysts with H_2 (H_2-TPR) were measured with a continuous flow reactor (BEL-TPD, Bel Japan Inc.) with a quadrupole spectrometer (MS) at the end of the reactor. A catalyst sample (20-50 mg) in a quartz glass reactor was pre-treated in O_2 at 500 ºC for 60 min and cooled down to 60 ºC in He. The sample was heated at a rate of 10 ºC min^{-1} to 750 ºC under a flow of 5%H_2/95%He, while monitoring the MS signal (m/e = 18, which is assignable to H_2O) for the outlet gas from the reactor.

Powder X-ray diffraction (XRD) patterns were recorded on an X-ray diffractometer (Mini Flex, Rigaku) with Cu Kα radiation (λ = 0.154 nm).

3. Results and Discussion

3.1. Comparison of catalytic performance of Ni/Al_2O_3 with those of unsupported Ni and Raney Ni.

Fig. 1 shows the time courses for the catalytic reduction of NO_3^- over 5 wt.% Ni/Al_2O_3, unsupported Ni, and Raney Ni. Fig. 1 also contains the result of bare Al_2O_3 without Ni. The products formed in the solution were NH_4^+ and NO_2^-, regardless of the catalysts and reaction conditions. As Fig. 1(a) shows, NO_3^- conversion was rapidly increased in early period of reaction time (~1 h) and reached to near 100% at 12 h. NH_4^+ was mainly formed in the solution and the formation of NO_2^- was negligibly small. For the bare Al_2O_3 (Fig. 1(b)), a sudden increase of NO_3^- conversion was observed within 1 h, but the conversion remained constant for further reaction time, while no product was detected in the solution over the reaction time. Since it is obvious that the bare Al_2O_3 does not have any catalytic activity for the reduction of NO_3^- under the present mild reaction conditions, it is reasonable that the sudden increase of NO_3^- conversion within 1 h was due to adsorption of NO_3^- on it. Thus, it is plausible that adsorption of NO_3^- on Al_2O_3 support caused the rapid increase of NO_3^- conversion in the reaction over 5 wt.% Ni/Al_2O_3. To confirm this, we carried out the reaction of NO_3^- under N_2 flow in the presence of 5 wt.% Ni/Al_2O_3 (Fig. 2). Under such reaction conditions, a similar

sudden increase of NO_3^- conversion was observed, but after that, the conversion did not change. After the gas was changed from N_2 to H_2 at 72 h, NO_3^- conversion was increased again with reaction time and NH_4^+ was formed. Therefore, we concluded that adsorption of NO_3^- occurred to increase the NO_3^- conversion suddenly in the early reaction time for the reduction of NO_3^- over 5 wt.% Ni/Al_2O_3.

In the case of unsupported Ni, the reduction of NO_3^- proceeded while the reaction rate was slow (Fig. 1(c)). The conversion of NO_3^- was only 55% at 12 h, which was far below that for 5 wt.% Ni/Al_2O_3 at the same reaction time. For Raney Ni, the conversion of NO_3^- jumped up to 80% at the early reaction time, but after that time the reaction did not proceed further. Since NH_4^+ and NO_2^- were formed in the solution, the reduction of NO_3^- occurred over Raney Ni. It is known that Raney Ni contains highly reactive hydrogen in its bulk, which is generated when Ni-Al alloy is activated in aqueous alkaline solution to obtain Raney Ni [48]. Assuming that the products other than NO_2^- and NH_4^+ was solely N_2, we estimated the amount of hydrogen required for the reduction of NO_3^- based on the conversion of NO_3^- (79%) and selectivities (9, 38 and 53% for NO_2^-, NH_4^+ and N_2, respectively at 12 h) and it was 3.75 mmol, which was almost the same as that of Ni in Raney Ni (0.2 g, 3.41 mmol) used for the reaction. This consistency implied that only hydrogen originally present in the Raney Ni was consumed for the reduction of NO_3^-, in other words, the reduction of NO_3^- with H_2 did not catalytically proceed under the reaction conditions. In the early papers on the catalytic reduction of NO_3^- over Raney Ni reported by Mikami et. al [44-46], the reaction experiment was performed with

a fixed-bed tubular flow reactor, in which gaseous H_2 and reaction solution alternately came to the catalyst bed and thus the catalyst (Raney Ni) was directly contacted with gaseous H_2, reducing the oxidized catalyst formed by the reaction with NO_3^-. In contrast, we carried out the reaction using a semi-batch reactor. In such a reactor, the catalyst was dispersed in the aqueous reaction solution and was reduced with H_2 dissolved in the reaction solution, meaning that the catalyst was contacted with very low concentration H_2, compared with gaseous 1 atm H_2. Such difference in the reactor system may be the reason why the catalytic reduction of NO_3^- did not proceed over the Raney Ni in this study.

Table 1 summarizes the reaction rates for NO_3^- reduction per unit weight of catalyst and per unit amount of Ni and selectivity to NH_4^+ over Ni/Al_2O_3 and the unsupported Ni. The result of Raney Ni was not included in Table 1 because, as mentioned above, only stoichiometric reduction of NO_3^- occurred under the present reaction conditions. To properly estimate the reaction rate, the data in the region where the NO_3^- conversion was increased monotonously with reaction time were used for the estimation (see Figs. S1(b), S2(b) and S3(b)). The reaction rate per unit weight of catalyst for Ni/Al_2O_3 was much faster than that for the unsupported Ni. Furthermore, the reaction rate per unit amount of Ni for 5 wt.% Ni/Al_2O_3 was the highest among the catalysts, being about twice as fast as 10 wt.% Ni/Al_2O_3 and hundred times as the unsupported Ni.

Comparing the selectivity at 24 h, the unsupported Ni showed the lowest one (Table. 1), but this was due to relatively low conversion of NO_3^-. In fact, Ni/Al_2O_3 showed selectivity to NH_4^+

comparable to the unsupported Ni when the selectivity was evaluated at around 70% conversion. From these results, we concluded that Ni/Al_2O_3 especially with 5 wt.% Ni loading was highly active Ni catalyst with the selectivity comparable to the unsupported Ni.

To further investigate the difference in the catalytic properties between Ni/Al_2O_3 and the unsupported Ni, we examined the influence of concentrations of NO_3^- ($[NO_3^-]_0$) and partial pressures of H_2 ($P(H_2)$). Fig. 3 shows time courses of NO_3^- conversion and product yields in the reduction of NO_3^- over 5 wt.% Ni/Al_2O_3 and the unsupported Ni with high $[NO_3^-]_0$ and low $P(H_2)$. The results under the standard reaction conditions ($[NO_3^-]_0$ = 400 ppm and $P(H_2)$ = 1.0 atm) shown in Fig. 3 are the same as those of Fig. 1(a) and 1(c) for 5 wt.% Ni/Al_2O_3 and the unsupported Ni, respectively. The reduction of NO_3^- proceeded even in high concentration of NO_3^- ($[NO_3^-]_0$ = 800 ppm) over 5 wt.% Ni/Al_2O_3. The reaction rate for NO_3^- reduction was 0.40 mmol h^{-1} $g_{cat.}^{-1}$ under the conditions, which was about twice of that for the reaction under the standard $[NO_3^-]_0$ (= 400 ppm).

On the other hand, the reaction with $P(H_2)$ = 0.75 atm over 5 wt.% Ni/Al_2O_3 showed an induction period up to 6 h. Mikami et al. reported that Raney Ni was gradually deactivated by the oxidation of the surface under the reaction conditions for the reduction of NO_3^- even though the reaction was performed in a fixed-bed tubular flow reactor [45, 46]. In addition, it is known that the surface of metallic Ni (Ni^0) is oxidized immediately by the exposure to air [49, 50]. From these facts, it is presumed that 5 wt.% Ni/Al_2O_3 was deactivated by the formation of the oxidized Ni surface, which

was formed by the contact with air, though we swiftly transferred the catalyst from the apparatus for the catalyst pretreatment to the reactor for the catalytic reaction. In fact, Ni 2p XPS spectrum for 5 wt.% Ni/Al_2O_3 exposed to air indicates the presence of the oxidized Ni species on the surface in addition to Ni^0 (Fig. S4). For the catalyst to show the catalytic activity, the oxidized surface layer should be reduced by the reaction with H_2. Under the reaction conditions with $P(H_2)$ = 1.0 atm, the reduction might proceed smoothly, since the induction period was short. However, it is considered that the rate for the reduction of the oxidized Ni species on the surface was slow with $P(H_2)$ = 0.75 atm. Therefore, it takes longer to exhibit the catalytic activity under such less reductive conditions.

The reaction behavior over the unsupported Ni was markedly different to that over 5 wt.% Ni/Al_2O_3 under the reaction conditions with high $[NO_3^-]_0$ and low $P(H_2)$ (Fig. 3(b)). The unsupported Ni turned to be rapidly deactivated at $P(H_2)$ = 0.75 atm. Furthermore, the conversion was not increased with prolonged reaction time in high $[NO_3^-]_0$ (= 800 ppm). The difference in the reaction behavior between 5 wt.% Ni/Al_2O_3 and the unsupported Ni strongly suggested that the active Ni species with different properties were presents on the catalysts, which will be discussed in detail in 3.2.

3.2. Structural difference between Ni/Al_2O_3 and unsupported Ni catalyst.

To reveal structures of the Ni species present on Ni/Al_2O_3 and the unsupported Ni, we measured powder XRD patterns of the catalysts before and after H_2 reduction (Fig. 4). In addition, we measured

H_2-TPR profiles for the catalysts before H_2 reduction (Fig. 5). The XRD patterns for Ni/Al_2O_3 before and after H_2 reduction shown in Fig. 4(c)–(f) are difference XRD patterns obtained by subtracting the pattern of bare Al_2O_3 from those of each Ni/Al_2O_3 sample. The original XPD patterns are given in Fig. S5.

The unsupported Ni before H_2 reduction exhibited the XRD pattern of NiO (Fig. 4(a)). In contrast, no diffraction line of NiO was observed for 5 wt.% Ni/Al_2O_3 before H_2 reduction, but broad diffraction lines assignable to $NiAl_2O_4$ phase were observed instead. For 10 wt.% Ni/Al_2O_3, the diffraction patterns of both NiO and $NiAl_2O_4$ were present before H_2 reduction.

After H_2 reduction, Ni metal (Ni^0) phase was commonly observed for all these samples. The unsupported Ni showed sharp diffraction lines of the Ni^0 phase and the mean size of the Ni^0 particles estimated by applying Scherrer's equation to the diffraction line at $2\theta = 44.4^o$ was 28 nm. On the other hand, the diffraction lines of the Ni^0 phase over Ni/Al_2O_3 were broad, especially for 5 wt.% Ni/Al_2O_3. The mean sizes of the Ni^0 particles for 5 and 10 wt.% Ni/Al_2O_3 were 8.4 and 9.5 nm, respectively, indicating that supporting Ni on Al_2O_3 formed smaller Ni^0 particles. No significant difference in the size of the Ni particles for 5 and 10 wt.% Ni/Al_2O_3 was also confirmed on the TEM images (Fig. S6). Notably, there was no shift in the diffraction angles of the Ni^0 phase for Ni/Al_2O_3, indicating that Al and other impurities were not incorporated in the Ni^0 particles.

The difference in the Ni species present on the catalysts before H_2 reduction caused that in behavior for the reduction with H_2 observed in H_2-TPR profiles (Fig. 5). Bare Al_2O_3 gave no reduction peak (Fig. 5(a)). The unsupported Ni had one reduction peak at 310 – 420 ºC (Fig. 5(b)), hereafter which is called the low temperature peak (L_{peak}). While there was no reduction peak in the temperature range of L_{peak} for 5 wt.% Ni/Al_2O_3, the broad reduction peak was observed above 450 ºC (Fig. 5(c)), hereafter which is called the high temperature peak (H_{peak}). Considering the results of XRD and H_2-TPR profiles, L_{peak} and H_{peak} were assignable to the reduction peaks of NiO and $NiAl_2O_4$, respectively.

According to the XRD patterns of the catalysts (Fig. 4), Ni existed only as the Ni^0 particles on the catalysts after H_2 reduction. However, it is expected that the Ni^0 particles formed by the reduction at low and high temperatures had different chemical and physical properties, governed by the extent of interaction with Al_2O_3 support. Such differences must be a cause of different catalytic properties between 5 wt.% Ni/Al_2O_3 and the unsupported Ni. Since the unsupported Ni was deactivated under the less reductive conditions, the Ni^0 particles formed by the low temperature H_2 reduction was hard to be reduced once it was deeply oxidized. On the other hand, the Ni^0 particles on 5 wt.% Ni/Al_2O_3 were relatively stable and easily regenerated with H_2 once the surface was oxidized.

10 wt.% Ni/Al_2O_3 after H_2 reduction had two types of Ni^0 particles; one was that similar to that on the unsupported Ni and the other was that on 5 wt.% Ni/Al_2O_3, since the catalyst showed both L_{peak}

and H_{peak} on the H_2-TPR profile. The catalytic properties of 5 and 10 wt.% Ni/Al_2O_3 will be compared and the difference will be discussed in detail later.

3.3. Reaction pathway for the reduction of NO_3^- over Ni/Al_2O_3.

For Pd-bimetallic catalysts including Pd-Cu and Pd-Sn, the reduction of NO_3^- sequentially proceeds through NO_2^- as an intermediate (Scheme 1(a)) [10]. Furthermore, it is demonstrated that the reaction of NO_3^- to NO_2^- is the rate-determining step. In fact, the reaction rate for the reduction of NO_2^- over Cu-Pd/AC was about three times faster than that of NO_3^- [15]. In order to investigate the reaction pathway for the reduction of NO_3^- over Ni/Al_2O_3, we performed the reduction of NO_2^- by using 5 wt.% Ni/Al_2O_3. As Fig. 6(a) shows, adsorption of NO_2^- on 5 wt.% Ni/Al_2O_3 occurred without giving any product formation in early reaction time. In addition, it should be noted that no reduction of NO_2^- proceeded even if the reaction time was further extended. This reaction behavior was completely different to that over the Pd-bimetallic catalysts.

Furthermore, we carried out the reaction in the mixed aqueous solution of NO_3^- and NO_2^- in the presence of 5 wt.% Ni/Al_2O_3 (Fig. 6(b)), in which concentration of each NO_2^- or NO_3^- was 3.23 mmol L^{-1} and thus the total concentration of the reactants (NO_3^- and NO_2^-) was the same as that of NO_2^- for the reaction shown in Fig. 6(a). Surprisingly, adsorption of only NO_2^- on the catalyst occurred, but that of NO_3^- did not do at all. In addition, no reduction of NO_3^- proceeded in the mixed solution. These

results indicated that NO_2^- strongly adsorbs on the Ni sites as well as Al_2O_3 surface on 5 wt.% Ni/Al_2O_3, causing catalyst poisoning once it forms during the reaction. Based on these results, it can be concluded that the reduction of NO_3^- did not proceed through NO_2^- over 5 wt.% Ni/Al_2O_3. This reaction pathway is quite different to that over the Pd-bimetallic catalysts. No formation of NO_2^- implies that the reduction of NO_3^- to adsorbed NO_2 through elimination of OH^- ($NO_3^- + 1/2H_2 \rightarrow NO_2(ad) + OH^-$) is the first step for the reaction over Ni/Al_2O_3 (Scheme 1(b)). Unfortunately, at present, there is no direct evidence for the formation of adsorbed NO_2 during the reaction and it is also unknown which step is rate-determining. Further study is absolutely necessary to elucidate the reaction mechanism and we will report it in the near future.

3.4. Influence of Ni loadings on the catalytic properties of Ni/Al_2O_3 for the reduction of NO_3^-.

As mentioned above, the unsupported Ni showed catalytic properties different from 5 wt.% Ni/Al_2O_3 for the reduction of NO_3^-, because the former had only the active Ni species formed by low temperature H_2 reduction, while the latter had only the one formed from $NiAl_2O_4$ at high temperature H_2 reduction. As the H_2-TPR profile demonstrates (Fig. 5(d)), 10 wt.% Ni/Al_2O_3 had both Ni species. Thus, it is expected that 10 wt.% Ni/Al_2O_3 shows the catalytic properties different from that of the unsupported Ni as well as 5 wt.%Ni/Al_2O_3. As Table 1 shows, the catalytic activity per unit amount of Ni for 10 wt.% Ni/Al_2O_3 under the standard reaction conditions ($[NO_3^-]_0$ = 400 ppm and $P(H_2)$ =

1.0 atm) was about half of that for 5 wt.% Ni/Al_2O_3, while the mean size of the Ni^0 particles on 10 wt.% Ni/Al_2O_3 was almost the same as that on 5 wt.% Ni/Al_2O_3. This implies that the catalytic activity of the Ni^0 particle formed by the high temperature H_2 reduction was much higher than that by the low temperature one.

Unlike the unsupported Ni, 10 wt.% Ni/Al_2O_3 showed the activity even at low $P(H_2)$ (= 0.5 – 0.75 atm) and high $[NO_3^-]_0$ (= 800 ppm) without any deactivation (Fig. S3). However, influence of $[NO_3^-]_0$ and $P(H_2)$ on the catalytic activity of 10 wt.%Ni/Al_2O_3 was markedly different to that of 5 wt.% Ni/Al_2O_3. In Fig. 7, the logarithm of conversion rates for NO_3^- are plotted as function of the logarithms of $[NO_3^-]_0$ in the range of 200 – 800 ppm and $P(H_2)$ in the range of 0.5 – 1.0 atm to estimate the reaction orders with respect to $[NO_3^-]_0$ and $P(H_2)$. From the slopes of the plots, the reaction orders were estimated to give eqs. 5 and 6 for 5 and 10 wt.% Ni/Al_2O_3, respectively.

$$r_{NO3-} = k_{(5\ wt.\%\ Ni)}[NO_3^-]^{0.8}P(H_2)^{0.8} \quad (5)$$

$$r_{NO3-} = k_{(10\ wt.\%\ Ni)}[NO_3^-]^{0}P(H_2)^{-0.2} \quad (6)$$

Assuming that the reduction of NO_3^- over 5 wt.% Ni/Al_2O_3 proceeded with a reaction mechanism that NO_3^- and H_2 competitively adsorb on Ni sites, adsorptions of both NO_3^- and H_2 on the Ni sites should be weak because of nearly first-order with respect to both $[NO_3^-]_0$ and $P(H_2)$ and thus the catalyst was not poisoned by strong adsorption of either NO_3^- or H_2.

In contrast, for 10 wt.% Ni/Al_2O_3, reaction orders with respect to $[NO_3^-]_0$ and $P(H_2)$ were 0 and –0.2, respectively. There are two plausible reaction mechanisms to explain such reaction orders, which are (i) NO_3^- and H_2 competitively adsorb on the Ni sites, and (ii) those do on the different Ni sites. If the former is possible, it is considered based on kinetics that H_2 preferentially occupied the Ni sites somewhat over NO_3^-. On the other hand, if the latter is more probable, both NO_3^- and H_2 strongly adsorb on the Ni sites. As mentioned before, 10 wt.% Ni/Al_2O_3 had at least two kinds of Ni^0 particles and thus the observed reaction data must be a sum of them occurred over each site, making the kinetic analysis more complicated. At present we do not know which mechanism in more possible. Thus, further mechanistic study must be necessary to clearly explain the kinetic data for Ni/Al_2O_3 with different Ni loadings.

Table 2 summarizes the selectivity to NH_4^+ for 5 and 10 wt.% Ni/Al_2O_3, taken from the reactions with different $[NO_3^-]_0$. For 5 wt.% Ni/Al_2O_3, the selectivity was about 45% regardless of $[NO_3^-]_0$. On the other hand, the selectivity to NH_4^+ seemed to decrease with increase in $[NO_3^-]_0$ for 10 wt.% Ni/Al_2O_3. As was explained with Scheme 1(b), gaseous nitrogen compounds (N_2 and N_2O) and NH_4^+ were formed with parallel reactions through NO and N species adsorbed on the Ni sites as intermediates. Thus, the gaseous nitrogen compounds likely form when the concentration of the adsorbed N species is high since two adsorbed N species (or adsorbed NO and N species) are necessary to form them, resulting in the decrease in the selectivity to NH_4^+. Therefore, the decrease in the

selectivity to NH_4^+ was observed for the reaction with high $[NO_3^-]_0$. As mentioned before, 10 wt.% Ni/Al_2O_3 had two kinds of the Ni sites formed by the low and high temperature H_2 reductions, whereas 5 wt.% Ni/Al_2O_3 had only the one formed by the high temperature H_2 reduction. The difference in the Ni sites present on 5 and 10 wt.% Ni/Al_2O_3 was also confirmed by the IR spectra of CO adsorbed on them (Fig. S7). Since 5 wt.% Ni/Al_2O_3 showed the constant selectivity independent of $[NO_3^-]_0$, the change in selectivity depending on $[NO_3^-]_0$ might occur on the Ni site formed by the low temperature H_2 reduction as present on 10 wt.% Ni/Al_2O_3.

4. Conclusions

In this study, the reduction of NO_3^- with H_2 in water over Ni/Al_2O_3 was performed and the catalytic performance was compared with that of the unsupported Ni. Ni/Al_2O_3 was superior in the activity to the unsupported Ni. The reaction rate for NO_3^- reduction over 5 wt.% Ni/Al_2O_3 was about 5 times and more than 100 times higher than that over the unsupported Ni, when those was compared by per unit weight of catalyst and per unit amount of Ni, respectively. In contrast to the unsupported Ni which was completely deactivated in low partial pressure of H_2 and high concentration of NO_3^-, Ni/Al_2O_3 was still active even under the less reductive conditions like $P(H_2)$ = 0.5 atm and $[NO_3^-]_0$ = 800 ppm. The unsupported Ni had the Ni^0 particles formed by the reduction of NiO with H_2 at 310 – 420 ºC, whereas 5 wt.% Ni/Al_2O_3 possessed the Ni^0 particles formed from $NiAl_2O_4$ by the reduction with H_2 above

450 ºC. Such difference in the reduction temperature gave the Ni^0 particles with different catalytic properties.

The Ni loadings for Ni/Al_2O_3 had a significant impact on the catalytic properties. The reaction orders with respect to both NO_3^- and H_2 were 0.8 for 5 wt.% Ni/Al_2O_3, while those were 0 and –0.2, respectively, for 10 wt.% Ni/Al_2O_3. On 10 wt.% Ni/Al_2O_3, there were two kinds of Ni^0 particles formed by low and high temperature H_2 reductions. The difference in the Ni^0 particles on Ni/Al_2O_3 with different Ni loadings caused the different catalytic properties between 5 and 10 wt.% Ni/Al_2O_3.

Unlike the previously reported Pd-bimetallic catalysts, the reduction of NO_3^- over Ni/Al_2O_3 did not proceed through NO_2^-. It is presumed that NO_3^- was reduced to adsorbed NO_2 through elimination of OH^- in the first-step.

Acknowledgements

This work was supported by JSPS KAKENHI Grant Number 18H017880.

References

[1] F.T. Wakida, D. N. Lerner, Water Res. 39 (2005) 3-16.

[2] L. Razowska-Jaworek, A. Sadurski (Eds.), Nitrate in Groundwater, A. A. Balkema Publishers, Leiden, 2005.

[3] World Health Organization, Guidelines for Drinking-water Quality, Forth edition (2011).

[4] F. Rezvani, M.-H. Sarrafzadeh, S. Ebrahimi, H.-M. Oh, Environ. Sci. Pollut. Res. 26 (2019) 1124-1141.

[5] A. Bhatnagar, M. Sillanpää, Chem. Eng. J. 168 (2011) 493-504.

[6] M. Chabani, A. Amrane, A. Bensmaili, Chem. Eng. J. 125 (2006) 111-117.

[7] J.A. Goodrich, B.W. Lykins Jr., R.M. Clark, J. Environ. Quality 20 (1991) 707-717.

[8] S. Tyagi, D. Rawtani, N. Khatri, M. Tharmavaram, J. Water Proc. Eng. 21 (2018) 84-95.

[9] S. Hörold, K.-D. Vorlop, T. Tacke, M. Sell, Catal. Today 17 (1993) 21-30.

[10] U. Prüsse, M. Hähnlein, J. Daum, K.-D. Vorlop, Catal. Today 55 (2000) 79-90.

[11] G. Strukul, R. Gavagnin, F. Pinna, E. Modaferri, S. Perathoner, G. Centi, M. Marcello, M. Tomaselli, Catal. Today 55 (2000) 139-149.

[12] M. Ilinitch, L.V. Nosova, V.V. Gorodetskii, V.P. Ivanov, S.N. Trukhan, E.N. Gribov, S.V. Bogdanov, F.P. Cuperus, J. Mol. Catal. A: Chem. 158 (2000) 237-249.

[13] H. Berndt, I. Mönnich, B. Lücke, M. Menzel, Appl. Catal. B: Environ. 30 (2001) 111-122.

[14] F. Epron, F. Gauthard, C. Pinéda, J. Barbier, J. Catal. 198 (2001) 309-318.

[15] U. Prüsse, K.-D. Vorlop, J. Mol. Catal. A: Chem. 173 (2001) 313-328.

[16] Y. Yoshinaga, T. Akita, I. Mikami, T. Okuhara, J. Catal. 207 (2002) 37-45.

[17] L. Lemaignen, C. Tong, V. Begon, R. Burch, D. Chadwick, Catal. Today 75 (2002) 43-48.

[18] A. Garron, K. Lázár, F. Epron, Appl. Catal. B: Environ. 59 (2005) 57-69.

[19] K. Nakamura, Y. Yoshida, I. Mikami, T. Okuhara, Chem. Lett. 34 (2005) 678-679.

[20] N. Barrabés, J. Just, A. Dafinov, F. Medina, J.L.G. Fierro, J.E. Sueiras, P. Salagre, Y. Cesteros, Appl. Catal. B: Environ. 62 (2006) 77-85.

[21] K. Nakamura, Y. Yoshida, I. Mikami, T. Okuhara, Appl. Catal. B: Environ. 65 (2006) 31-36.

[22] I. Brahim, D.P. Barbosa, M.C. Rangel, F. Epron, Appl. Catal. B: Environ. 93 (2009) 50-55.

[23] J.K. Chinthaginjala, L. Lefferrts, Appl. Catal. B: Environ. 101 (2010) 144-149.

[24] L. Calvo, M.A. Gilarranz, J.A. Cases, A.F. Mohedano, J.J. Rodriguez, Ind. Eng. Chem. Res. 49 (2010) 5603-5609.

[25] Y. Xie, H. Cao, Y. Li, Y. Zhang, J.C. Crittenden, Environ. Sci. Technol. 45 (2011) 4066-4072.

[26] A. Devadas, S. Vasudevan, F. Epron, J. Hazard. Mater. 185 (2011) 1412-1417.

[27] K. Wada, T. Hirata, S. Hosokawa, S. Iwamoto, M. Inoue, Catal. Today 185 (2012) 81-87.

[28] J. Jung, S. Bae, W. Lee, Appl. Catal. B: Environ. 127 (2012) 148-158.

[29] Z. Gao, Y. Zhang, D. Li, C. J. Werth, Y. Zhang, X. Zhou, J. Hazard. Mater. 286 (2015) 425-431.

[30] S. Hamid, M.A. Kumar, W. Lee, Appl. Catal. B: Environ. 187 (2016) 37-46.

[31] J. Hirayama, Y. Kamiya, Catal. Sci. Technol. 8 (2018) 4985-4993.

[32] X. Huo, D.J.V. Hoomissen, J. Liu, S. Vyas, T.J. Strathmann, Appl. Catal. B: Environ. 211 (2017) 188-198.

[33] D.L. Trimm, Design of Industrial Catalysts, Elsevier, North-Holland, 1980, 169.

[34] J.M. Thomas, W.J. Thomas, Principles and Practice of Heterogeneous Catalysis, VCH Verlagsgellschaft mbH, Weinheim, 1997, 540-544.

[35] R.J. Farrauto, C.H. Bartholomev, Fundamentals of Industrial Catalytic Processes, Chapman & Hall, London, 1997, 415-418.

[36] C.H. Bartholmew, R.J. Farrauto, Fundamentals of Industrial Catalytic Processes, Second ed., John Wiley & Sons, Hoboken, 2006, 524-531.

[37] I. Mikami, T. Okuhara, Chem. Lett. 31 (2002) 932-933.

[38] I. Mikami, Y. Yoshinaga, T. Okuhara, Appl. Catal. B: Environ. 49 (2004) 173-179.

[39] I. Mikami, R. Kitayama, T. Okuhara, Appl. Catal. A: Gen. 297 (2006) 24-30.

[40] O.S.G.P. Soares, J.J.M. Órfão, M.F.R. Pereira, Catal. Lett. 126 (2008) 253-260.

[41] B.C. Gates, Catalytic Chemistry, John Wiley & Sons, Inc., New York, 1992, pp.378-396.

[42] J.A. Anderson, M.F. García (Eds.), Supported Metals in Catalysis, Imperial College Press, 2005.

[43] T. Mitsudome, Y. Mikami, M. Matoba, T. Mizugaki, K. Jitsukawa, K. Kaneda, Angew. Chem. Int. Ed. 51 (2012) 136-139.

[44] C. Jiang, K. Hara, A. Fukuoka, Angew. Chem. Int. Ed. 52 (2013) 6265-6268.

[45] Y. Yazawa, H. Yoshida, N. Takagi, S. Komai, A. Satsuma, T. Hattori, J. Catal. 187 (1999) 15-23.

[46] A. Taketoshi, M. Haruta, Chem. Lett. 43 (2014) 380-387.

[47] J. Petró, A. Bóta, K. László, H. Beyer, E, Kálmán, I. Dódony, Appl. Catal. A: Gen. 190 (2000) 73-86.

[48] H.A. Smith, A.J. Chadwell, S.S. Kirslis, J. Phys. Chem. 59 (1955) 820-822.

Table 1 Reaction rate and selectivity to NH_4^+ over various Ni catalysts for catalytic reduction of NO_3^- in water.

Catalysts	Reaction rate[a]		NH_4^+ selectivity / %
	/ mmol h^{-1} $g_{cat.}^{-1}$	/ mol h^{-1} mol_{Ni}^{-1}	
5 wt.%Ni/Al_2O_3	0.21	0.24	48[b] (31)[c]
10 wt.%Ni/Al_2O_3	0.22	0.13	36[b] (33)[c]
Unsupported Ni	0.04	0.002	26[b]

Reaction conditions: catalyst weight, 0.2 g; $[NO_3^-]_0$ = 400 ppm; volume of reaction solution, 120 mL; H_2 flow rate, 30 mL min^{-1}; $P(H_2)$ = 1.0 atm and reaction temperature, 40 ºC. [a] The reaction rates were calculated from the slopes of the conversion-time curves shown in Figs. S1 (b), S2 (b) and S3 (b). [b] The values at 24 h, at which the conversion of NO_3^- was almost 100% for Ni/Al_2O , while 73% for unsupported Ni. [c] The conversion of NO_3^- was around 70%.

Table 2 Comparison of NH_4^+ selectivity between 5 and 10 wt%. Ni/Al_2O_3 in the catalytic reduction of NO_3^- with H_2 in water.

Catalyst	$[NO_3^-]_0$ / ppm	NH_4^+ selectivity[a] / %
5 wt.% Ni/Al_2O_3	200	45
	400	48
	800	42
10 wt.% Ni/Al_2O_3	200	72
	400	36
	800	35[b]

[a] Selectivity to NH_4^+ at 100% conversion of NO_3^- (see Figs. S1 and S3).

[b] Selectivity to NH_4^+ at 95% conversion of NO_3^- (see Figs. S3).

(a) Pd-bimetallic catalyst

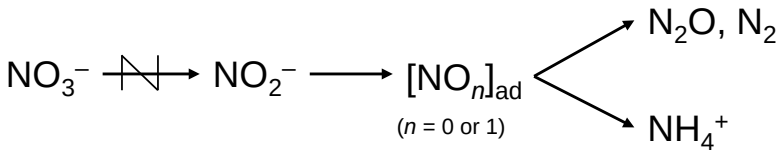

(b) Supported Ni catalyst

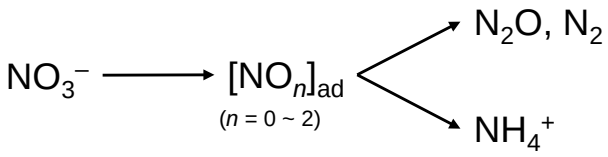

Scheme 1 Reaction pathways for catalytic reduction of NO_3^- with H_2 over (a) Pd-bimetallic catalyst and (b) supported Ni catalyst.

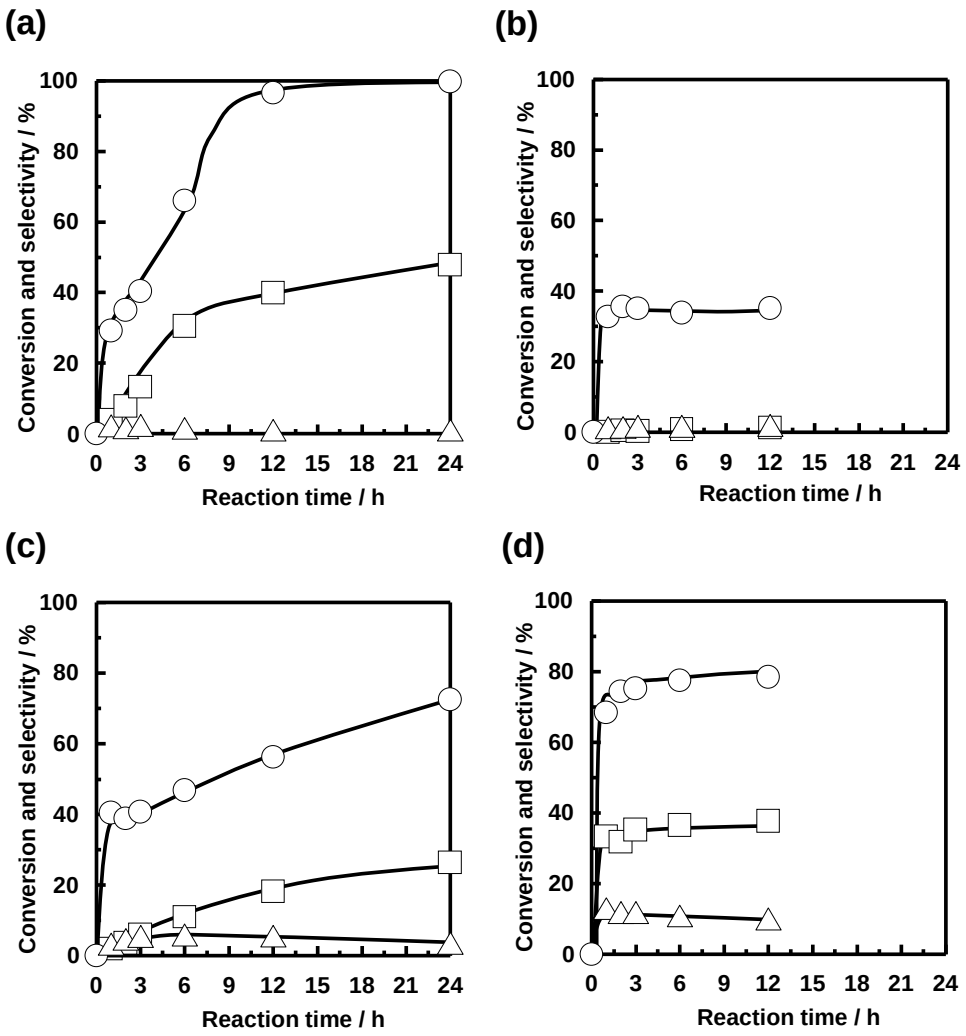

Fig. 1 Time courses of conversion of NO_3^- and selectivities to NO_2^- and NH_4^+ in catalytic reduction of NO_3^- in water over (a) 5 wt.% Ni/Al_2O_3, (b) bare Al_2O_3, (c) unsupported Ni and (d) Raney Ni. (○) Conversion of NO_3^- and selectivities to (△) NO_2^- and (□) NH_4^+. Reaction conditions: catalyst weight, 0.2 g; $[NO_3^-]_0$ = 400 ppm; volume of reaction solution, 120 mL; H_2 flow rate, 30 mL min^{-1}; $P(H_2)$ = 1.0 atm; and reaction temperature, 40 ºC.

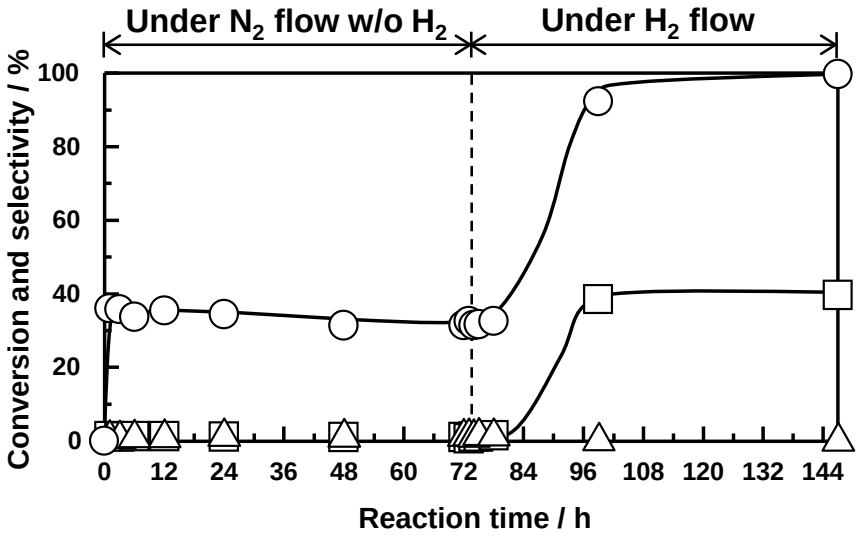

Fig. 2 Sequential reaction of NO_3^- over 5 wt.% Ni/Al_2O_3 under N_2 flow (0 – 72 h) and H_2 flow (72 – 144 h). (○) Conversion of NO_3^- and selectivities to (△) NO_2^- and (□) NH_4^+. Reaction conditions: catalyst weight, 0.2 g; $[NO_3^-]_0$ = 400 ppm; volume of reaction solution, 120 mL; gas flow rate, 30 mL min^{-1}; $P(N_2)$ or $P(H_2)$ = 1.0 atm; and reaction temperature, 40 ºC.

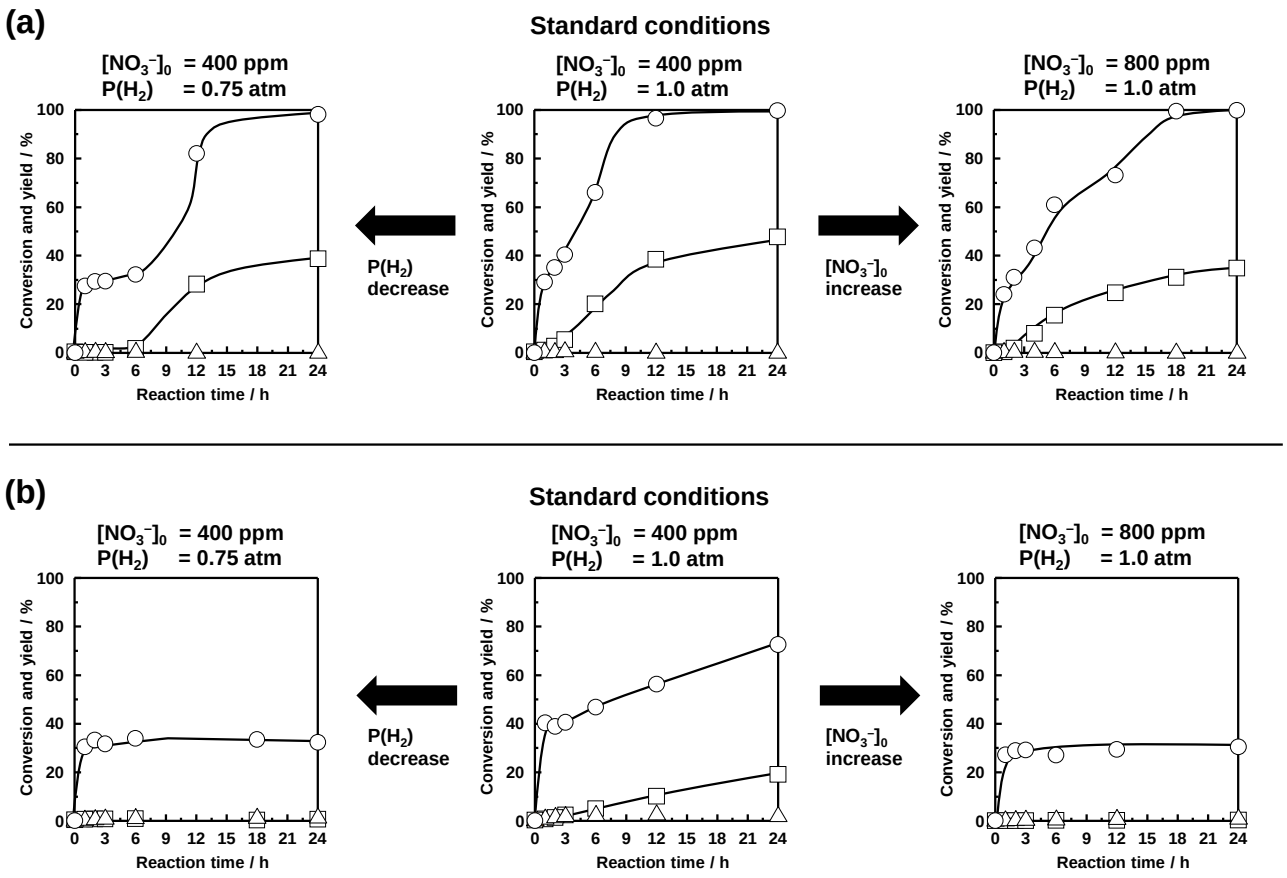

Fig. 3 Influence of initial concentrations of NO_3^- ($[NO_3^-]_0$) and partial pressures of H_2 ($P(H_2)$) on reduction of NO_3^- in water over (a) 5 wt.% Ni/Al_2O_3 and (b) unsupported Ni. (○) Conversion of NO_3^- and yields of (△) NO_2^- and (□) NH_4^+. Reaction conditions: catalyst weight, 0.2 g; volume of reaction solution, 120 mL; gas flow rate, 30 mL min^{-1}; and reaction temperature, 40 ºC.

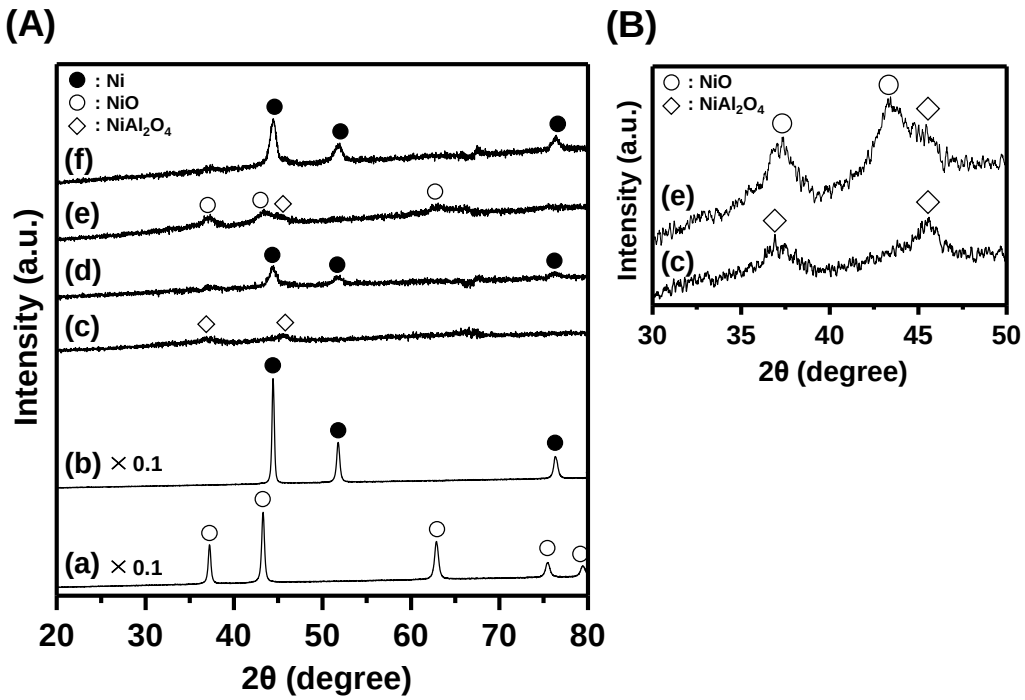

Fig. 4 XRD patterns of (a) unsupported Ni before H_2 reduction, (b) unsupported Ni after H_2 reduction, (c) 5 wt.% Ni/Al_2O_3 before H_2 reduction, (d) 5 wt.% Ni/Al_2O_3 after H_2 reduction, (e) 10 wt.% Ni/Al_2O_3 before H_2 reduction, and (f) 10 wt.% Ni/Al_2O_3 after H_2 reduction. (c)-(f): Diffraction patterns obtained by subtracting that of Al_2O_3 from each of them. (A) wide and (B) narrow 2θ ranges.

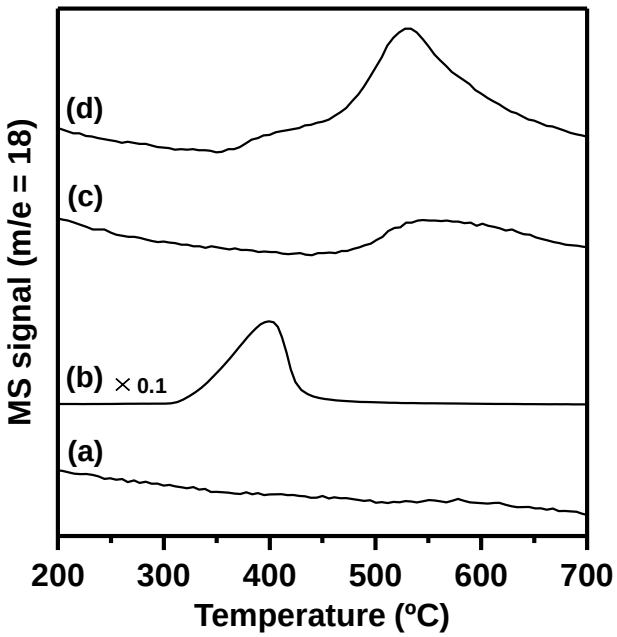

Fig. 5 H_2-TPR profiles of (a) bare Al_2O_3, (b) unsupported Ni, (c) 5 wt.% Ni/Al_2O_3 and 10 wt.% Ni/Al_2O_3.The TPR profiles were taken for the samples before H_2 reduction

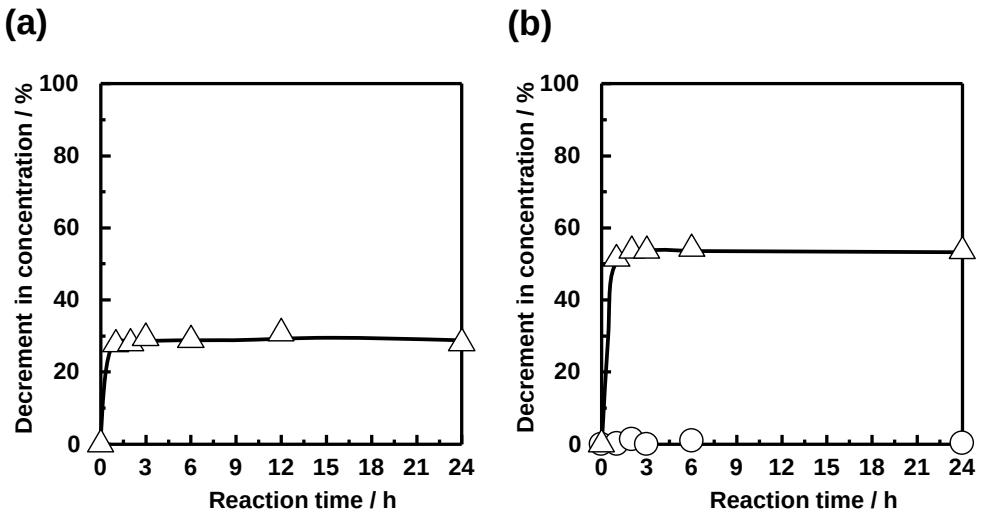

Fig. 6 Reaction of NO_2^- in water over 5 wt.% Ni/Al_2O_3 (a) in the absence and (b) in the presence of NO_3^-. Conversions of (△) NO_2^- and (○) NO_3^-. Reaction conditions: catalyst weight, 0.2 g; reactant (a) $[NO_2^-]_0$ = 400 ppm = 6.46 mmol L^{-1} and (b) $[NO_3^-]_0$ = 3.23 mmol L^{-1} + $[NO_2^-]_0$ = 3.23 mmol L^{-1}; volume of reaction solution, 120 mL; H_2 flow rate, 30 mL min^{-1}; and reaction temperature, 40 ºC.

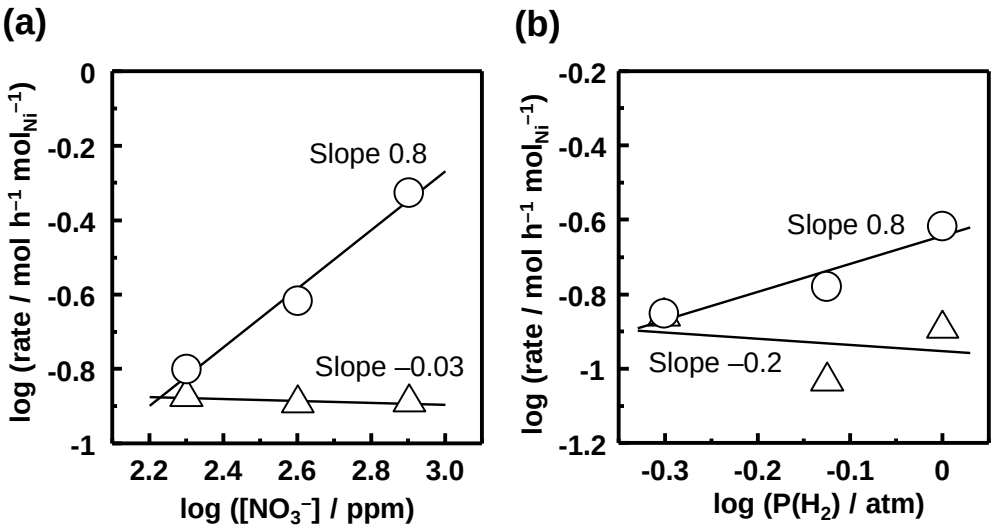

Fig. 7 Dependence of NO_3^- decomposition rates on (a) initial concentrations of NO_3^- ($[NO_3^-]_0$) and (b) partial pressures of H_2 ($P(H_2)$) for catalytic reduction of NO_3^- over (○) 5 wt.%Ni/Al_2O_3 and (△) 10 wt.%Ni/Al_2O_3. Reaction conditions: catalyst weight, 0.2 g; $[NO_3^-]_0$ = 200-800 ppm; volume of reaction solution, 120 mL; H_2 gas flow rate, 30 mL min^{-1}; $P(H_2)$ = 0.5-1.0 atm; and reaction temperature, 40 ºC.